Available online at www.sciencedirect.com
ScienceDirect
Journal of the European Ceramic Society 30 (2010) 181–186
www.elsevier.com/locate/jeurceramsoc

Controlled growth of anodic aluminium oxide films with hexagonal array of nanometer-sized pores filled with textured copper nanowires

R. Bertholdo, M.C. Assis, P. Hammer, S.H. Pulcinelli, C.V. Santilli *

São Paulo State University, IQ/UNESP, P.O. Box 355, 14800-900, Araraquara, SP, Brazil

Available online 8 July 2009

Abstract

Anodic aluminium oxide (AAO) films exhibiting a homogeneous morphology of parallel pores perpendicular to the surface were prepared in a two-step anodization process and filled with copper by electrochemical deposition. The optimum growth conditions for the formation of free-standing AAO films with hexagonal compact array of cylindrical pores were studied by field emission scanning electron microscopy and small angle X-ray scattering. The results show well-defined periodic structures with uniform pores size distribution for films with pore diameters between 40 and 70 nm prepared using different voltages and temperatures during the second anodization step. X-ray photoelectron spectroscopy and X-ray diffraction analysis of AAO films filled with copper show the formation of nanowires with high structural order, exhibiting a preferential crystalline orientation along the (2 2 0) axis and only small fraction of copper oxides. The best results for textured Cu nanowires were obtained at a reduction potential of −300 mV.

Keywords: Anodic alumina films; Self-organized pore arrays; Copper nanowires; Structural properties

1. Introduction

The variety of distinct properties of one-dimensional (1D) nanostructured materials based on quantum size effects,[1] have attracted considerable attention in the field of material science. Carbon nanotubes and metallic nanowires are two typical nanostructures presenting unique physical and chemical properties.[2,3] An emerging method to prepare these nanomaterials, designated "template synthesis",[4] is based on a porous matrix which defines the dimension and determines the growth direction of the 1D nanostructures. Among the ceramic templates, the anodic aluminium oxide (AAO) films presenting an ordered array of cylindrical pores with nanometric diameter, are most commonly used due to the simple electrochemical processing of the self-organized structure.[5] AAO films have also been used as membranes in filtration process,[6] 2D photonic crystals[7] and chemical biosensors.[8] On the other hand, using AAO films, the electrochemical deposition process is an attractive synthesis route for 1D nanostructures, providing a controllable and inexpensive method for the preparation of metallic nanowires with well-defined geometry.[9] The synthesized nanomaterial can be used for various applications such as anisotropic electrical and thermal conductor in the form of ceramic-nanowire arrays or as interconnections in nanoscaled electronic circuits, nanosensors or electron emitters produced from bundles of nanowires, which can be obtained by selective dissolution of the ceramic template in an adequate chemical process.[10]

Although the AAO films with an amorphous pore structure can be produced in a quite large parameters range without substantial change in morphology, the self-organized arrangement of neighbouring pores in highly regular polycrystalline hexagonal array occurs only for a quite small processing window. Thus, in order to achieve control of the structural ordering in the form of a hexagonal array of close-packed cylindrical pores and of the grown nanowires it is crucial to identify and to understand in detail the relationship between preparation parameters and structural features of the porous template.

Therefore, this work focuses on the effect of electrolyte temperature and anodization voltage on the structural features of AAO films presenting a polycrystalline hexagonal array of cylindrical nanopores with controlled diameter. These films were used as template to confine the growth of copper nanowires inside the cylindrical nanopores. Scanning electron microscopy (SEM) and small angle X-ray scattering (SAXS) were used to study the morphology and nanostructure of the AAO films, while X-ray photoelectron spectroscopy (XPS) and X-ray powder diffraction

* Corresponding author. Tel.: +55 1633016645; fax: +55 1633016692.
E-mail address: santilli@iq.unesp.br (C.V. Santilli).

0955-2219/$ – see front matter © 2009 Elsevier Ltd. All rights reserved.
doi:10.1016/j.jeurceramsoc.2009.06.014

(XPRD) analysis were applied to analyse the composition and crystalline structure of copper nanowires.

2. Experimental

The anodic aluminium oxide membranes were synthesized in a two-step anodization process.[11] An aluminium foil (99.99%, Alfa Aesar) of 100 μm thickness was rinsed by acetone, ethanol, deionized water and dried in air stream. This specimen was used as anode and a platinum foil with the same circular area as cathode (1.5 cm^2). The distance between the cathode and the anode was fixed at 40 mm. A magnetic stirred 0.3 mol L^{-1} aqueous oxalic acid solution was used as electrolyte. The first anodization was performed at different dc voltages (30, 40 and 50 V) during 2.5 h, maintaining the electrolyte temperature constant at 5, 15 and 25 °C. The resulting oxide film was selectively dissolved in a mixture of 120.7 g L^{-1} phosphoric and 18.3 g L^{-1} chromic acids at 60 °C. The second anodization step was performed at the same conditions for a period of 30 min. Finally the non-anodized aluminium was removed with a saturated tin tetrachloride aqueous solution, resulting in free-standing AAO films with a thickness of about 10 μm.

The electrochemical deposition of copper nanowires was carried out from a 0.2 mol L^{-1} $CuSO_4$ solution at pH = 4 at room temperature using a potentiostatic technique. A 200 nm thickness Au film deposited by sputtering on the backside of the AAO film was used as cathode. It was attached to the electrochemical cell equipped with two Pt counter electrodes and an Ag/AgCl reference electrode. The reduction overpotential was varied between −100 and −300 mV with an increment of 50 mV.

The structural parameters of the AAO films were evaluated by field emission scanning electron microscopy (SEM) using a JEOL, JSM-6330F microscope, and by small angle X-ray scattering (SAXS) measurements. SAXS experiments were performed at the SAXS beamline of the National Synchrotron Light Laboratory (LNLS, Campinas, Brazil). The beamline is equipped with an asymmetrically cut and bent silicon (1 1 1) monochromator that yields a monochromatic and focused beam (λ = 1.488 Å). A bi-dimensional position-sensitive X-ray detector was used to record the scattering intensity, $I(q)$, as a function of the modulus of scattering vector $q = (4\pi/\lambda)\sin\theta$, θ being half the scattering angle. The AAO film was oriented perpendicularly to the incident beam, so that the mean pore axis was parallel to the beam axis.

The morphology, nature of crystalline phases and composition of the nanowires were investigated as a function of the reduction potential by SEM, X-ray powder diffraction (XRPD), using the Cu K_α radiation selected by a curved graphite monochromator (Siemens D5000), and X-ray photoelectron spectroscopy (UNI-SPECS UHV). The XPS analysis was carried out at the backside of the membrane after removing the gold layer. The Mg K_α line was used ($h\nu$ = 1253.6 eV) and the analyser pass energy was set to 10 eV for the measurement of the high resolution Cu 2p, Cu LMM, Al 2p, O 1s and C 1s core level spectra. The inelastic background of the spectra was subtracted using Shirley's method and the binding energies were corrected using the hydrocarbon component of adventitious carbon fixed at 285.0 eV. The composition of the surface layer was determined from the ratio of the relative peak areas corrected by sensitivity factors of the corresponding elements. The spectra were fitted without placing constraints using multiple Voigt profiles.

3. Results and discussion

In the two-step anodization process to form AAO membranes, the pore arrangement is defined by the first anodization step while the pore length depends on the duration of the second anodization process.[11] The self-organization of the pores to form a hexagonal array can be explained by a repulsive interaction between pores, characterized by a higher local electric field, and by the chemical dissolution at the oxide/electrolyte interface.[12] In this process, the quality of the structure depends strongly on both the electrolyte temperature and the anodization voltage. The effect of these parameters on the porous structure of AAO films is displayed in the SEM images of Fig. 1. A compact array of pores within crystalline domains is verified for all samples. At low voltages or low temperatures the presence of small pores forming not only ordered domains with a hexagonal structure is observed, but also less ordered regions are clearly visible. Several kinds of defects were found in these less ordered domains, such as deviation from circular symmetry, pore vacancy and localized absence of walls due to the pore coalescence. At high voltages or temperatures, a higher regularity of the hexagonal array of pores can be observed. The average values of the pore diameter D_p and of the interpore distance D_{int}, estimated from these images analysis are displayed in columns two and three of Table 1. In agreement with the results reported for AAO films produced at higher voltages (>100 V), both D_p and D_{int} increased with the anodization potential.[13] In contrast, increasing the electrolyte temperature, the interpore distance remains essentially unchanged, while the pore diameter increases. These results clearly evidence that the anodization potential determines the value of D_{int}, while the increase of the electrolyte acidity with temperature enhances the dissolution of the pore walls and consequently, the growth of the pore diameter.

Considering that the entire volume of the X-ray irradiated area is probed in the SAXS measurement, a more representative structural description of the AAO films can be obtained from the scattering pattern displayed in Fig. 2. The bi-dimensional SAXS scattering pattern (insert in Fig. 2(b)) of all samples exhibits uniform intensities along the rings at a scattering vector radius equal to q_{hk} ($h\,k$ is the Miller Index of the bi-dimensional lattice with $l = \infty$). The observed patterns correspond to scattering by a polycrystalline system with correlation size of several lattice constant. These isotropic bi-dimensional patterns were radially averaged to yield one-dimensional $I(q)$ profiles plotted in Fig. 2(a) and (b) for samples prepared at several electrolyte temperatures and anodization voltages, respectively. No significant changes of the peak positions occur for different anodization temperatures (Fig. 2(a)). As the $D_{int} \approx 95$ nm, determined by SEM, corresponds to a q_{10} value equal to 0.076 nm^{-1} it was not possible to probe completely the (1 0) reflection of the hexagonal lattice with the experimental SAXS setup used in this measurement, allowing a minimum q value of 0.08 nm^{-1}. Thus the two

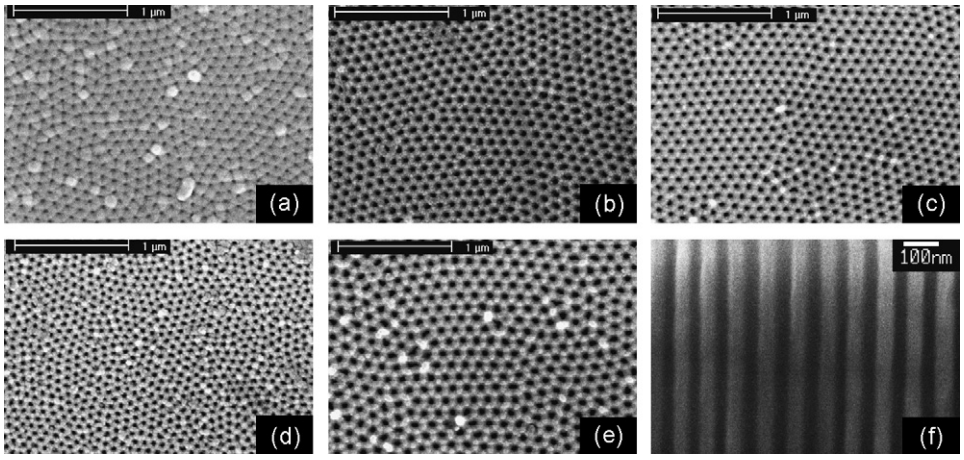

Fig. 1. Top-view SEM images of AAO film synthesized at 40 V and different temperatures (a) 5 °C, (b) 15 °C, (c) 25 °C, and at 15 °C applying (d) 30 V, (b) 40 V and (e) 50 V. (f) Cross-section of the AAO film grown at 40 V and 15 °C.

intense peaks observed in the pattern of Fig. 2(a) were indexed as (1 1) and (3 1) reflections, for which the expected $q_{11}/q_{31} = 1/2$ ratio for a hexagonal lattice is satisfied. Since the D_{int} is essentially independent of the electrolyte temperature, the position of the diffraction peaks are equal for all samples. In contrast, the position of peaks corresponding to given $h\,k$ families shifts to smaller wave vector modulus values with increasing anodization potential (Fig. 2(b)). Note the presence of the (1 0) reflection in the SAXS profile of sample anodized at 30 V.

The values of the lattice parameter of the hexagonal cell (a_{hex}), calculated from the reciprocal lattice vectors, q_{hk} ($a_{hk} = 4\pi(h^2 + h\,k + k^2)^{1/2}/(q\sqrt{3})$) are presented in the column four of Table 1. The good agreement found between the D_{int} and a_{hex} indicates that the results obtained from the SEM analysis of the top surface are representative for the entire volume of the AAO film. Under this condition the porosity of the hexagonal structure can be estimated from the ratio between the pore radius (r) and D_{int} as $P = (2\pi/\sqrt{3})(r/D_{int})^2$. The columns five and six of Table 1 compare the porosity values with the crystallite size ($L_C = 4\pi/\beta$) calculated from the half maximum broadening (β) of the (3 1) peak after separation of the (4 0) reflection using two pseudo-Voigt functions. Although the quite different anodization conditions result in different D_p and D_{int} values, larger crystallites are obtained for samples with about 10% porosity. This finding indicates that $P \approx 10\%$ is the most favourable condition for the formation of a ordered hexagonal porous structure. This observation is in agreement with the predictions of the mechanical stress model for the self-ordered pore growth of AAO films.[14] According to this model, the stress intensity resulting from the volume expansion involved in the formation of porous alumina layer determines the intensity of the force promoting the pore ordering. The linear strain (ξ) resulting from this expansion is maximum for a non-porous alumina layer and it decreases with increasing porosity. For $P > 10\%$ ($\xi < 1.2$) the compressive stress is too small to promote pore ordering, while for $P < 10\%$ ($1.3 < \xi < 2$) the stress is high enough to promote the shrinkage of the initial pore and the densification of the alumina layer. Thus only for $P \approx 10\%$, corresponding to $\xi \approx 1.2$, the best ordered pore structure will grow.

The as-prepared AAO films were used as template to direct the growth of copper nanowires during the electrochemical deposition process. A typical SEM cross-section image of copper nanowires deposited at −250 mV inside the pores of the AAO film (Fig. 1(f)) is displayed in Fig. 3. The image shows that the individual nanowires are homogenous and continuous. It should be pointed out that there is no obvious difference in the nanowire morphology in the range of the applied potential, the main difference is the varying degree of filling of the pores due to competing copper film formation on de upper side of the AAO membrane.

The crystalline structure of the copper nanowires deposited in the overpotential range from −100 to −300 mV was analyzed by XRPD. For all samples, a mixture of metallic Cu and copper oxide was found, with a fraction of Cu_2O varying

Table 1
Structural parameters of the AAO samples obtained from SEM and SAXS measurements.

Parameter		D_p (nm)	D_{int} (nm)	a_{hex} (nm)	$P \pm 3$ (%)	$L_C \pm 10$ (nm)
Temperature (°C)	5	17 ± 3	95 ± 7	105 ± 1	3	360
	15	42 ± 3	94 ± 11	105 ± 2	18	370
	25	31 ± 3	95 ± 7	105 ± 1	10	450
Anodization potential (V)	30	28 ± 6	71 ± 10	80 ± 1	14	285
	40	42 ± 3	94 ± 11	105 ± 1	18	370
	50	39 ± 6	109 ± 15	128 ± 1	12	480

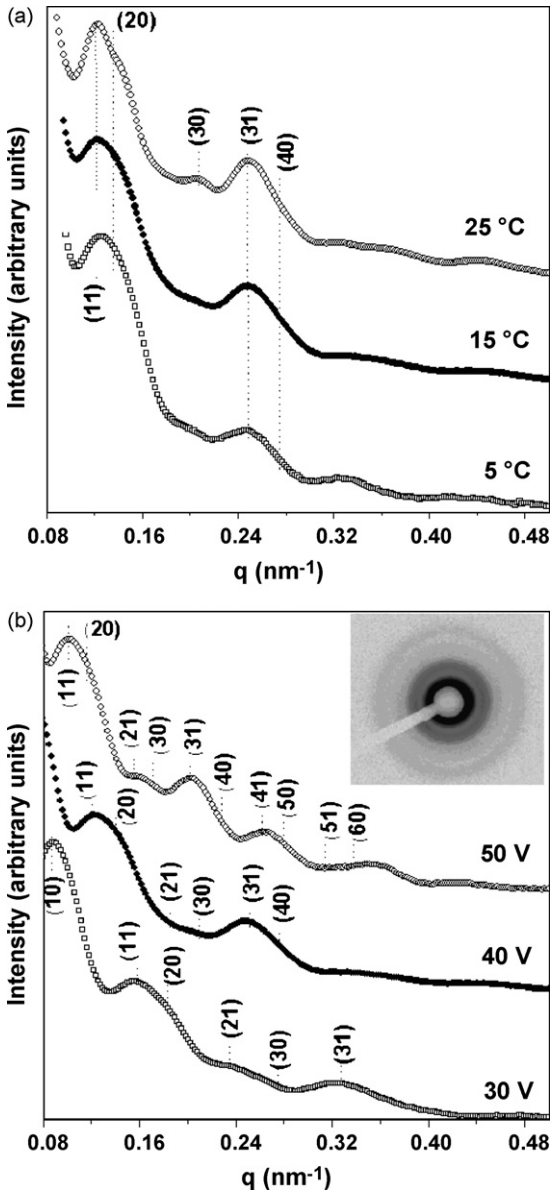

Fig. 2. Small angle X-ray scattering curves for AAO films prepared at different (a) temperatures and (b) anodization voltages.

with the deposition voltage. For samples prepared at overpotentials equal or lower than −150 mV, polycrystalline copper oxides (Cu_2O and CuO) were found as predominant phases, showing intensities and positions of the diffraction peaks in agreement with those expected for randomly oriented polycrystalline phases with cubic face-centred structure. On the other hand, higher overpotentials favour the formation of the metallic Cu phase. XRPD patterns corresponding to samples prepared at −200, −250 and −300 mV containing different Cu_2O amounts are shown in Fig. 4. The relative intensities of reflections indexed as (1 1 1), (2 2 0), (2 2 0) and (3 1 1) indicate a preferential orientation of the metallic Cu phase along the (2 2 0) direction.

Quantitative information concerning the preferential crystallite orientation was obtained from the texture coefficient, T_C, defined as: $T_C = (I_{hkl}/I^R_{hkl})/(1/n\sum(I_{hkl}/I^R_{hkl}))$, where n is the number of the diffraction peaks, I_{hkl} and I^R_{hkl} denote the integrated intensities corresponding to ($h\,k\,l$) reflections of samples containing textured and randomly oriented grains, respectively. The value $T_C = 1$ represents films with randomly oriented crystallites, while higher values indicate the abundance of grains oriented in a given ($h\,k\,l$) direction. Considering the four main peaks ($n = 4$) of the cubic Cu^0 lattice a maximum value of $T_C = 4$ can be reached for a completely textured sample. The T_C data presented in Table 2 show that samples prepared at −250 and −300 mV are almost entirely textured in the (2 2 0) direction. Furthermore, Table 2 shows that the ratio of the integrated peak intensities $I_{Tot}(Cu^0)/I_{Tot}(Cu_2O)$ increases for higher overpotential, indicating a dominating presence of the metallic phase. For these samples a grain size of about 85 nm was determined from the half maximum broadening of the (2 2 0) line of Cu^0, using the Scherrer formula.

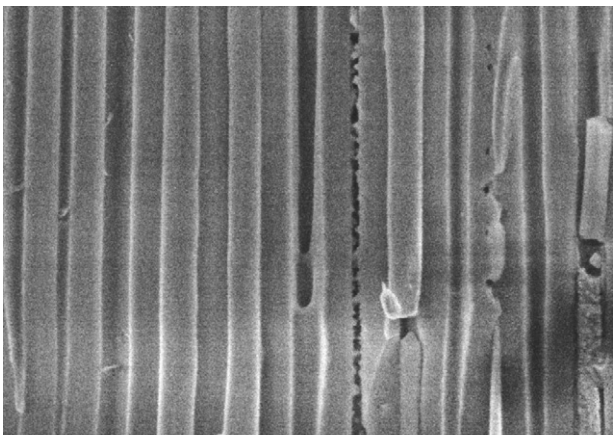

Fig. 3. Representative SEM cross-sectional image of copper nanowires deposited at −250 mV inside the nanochannels of the AAO film. The observed fragments were caused by the cutting process.

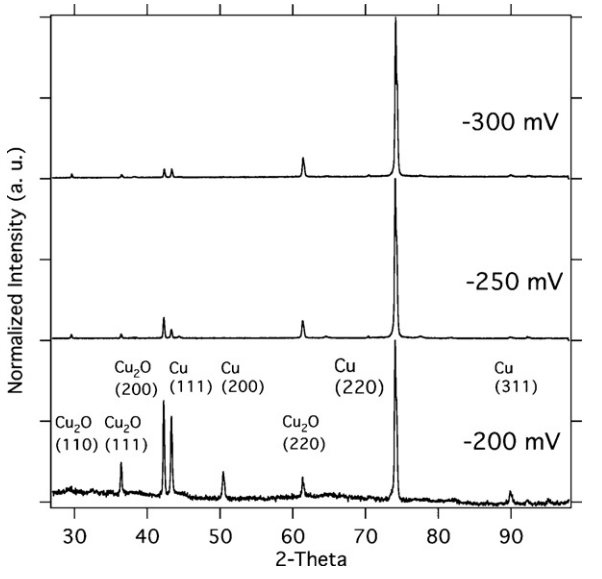

Fig. 4. XRPD patterns of the AAO film showing the presence of highly textured Cu and Cu_2O phases for nanowires deposited at −200, −250 and −300 mV.

Table 2
Texture coefficient T_C for the Cu (2 2 0) direction and the ratio of the integrated peak intensities, $I_{Tot}(Cu)/I_{Tot}(Cu_2O)$, as a function of the deposition potential.

Overpotential (mV)	T_C Cu (2 2 0)	$I_{Tot}(Cu)/I_{Tot}(C_2O)$
−100	–	0.0
−150	1.2	2.0
−200	3.1	1.8
−250	3.9	4.1
−300	3.9	5.4

The quantitative XPS analysis of the surface region of the as-prepared AAO film confirmed the stoichiometry of the Al_2O_3 phase and the absence of metallic Al (not shown). The existence of copper oxides in most of the samples was confirmed by the structural analysis of the XPS data. A particular attention was given to the textured samples deposited at −250 and −300 mV studying the core level spectra from data collected at the bottom side of the template after Au removal. As shown in the Cu $2p_{3/2}$ spectrum displayed in Fig. 5 for nanowires grown at −300 mV, besides a small fraction of CuO and $CuSO_4$ identified at 935.5 and 933.7 eV, respectively, the main component at 932.5 eV can be assigned to the presence of Cu^0 (932.7 ± 0.3 eV) and Cu_2O (932.5 ± 0.3 eV).[15] Due to the difficulty to separate the contributions of these phases in the photoemission spectrum, the Auger $L_3M_{45}M_{45}$ peak was recorded to determine the Cu^0 to Cu_2O ratio.

In agreement with the XRPD results, the differentiated Auger spectra (insert Fig. 5) reveal that the main part of the textured copper phase deposited at −300 mV is related to metallic Cu, with the peak located at a kinetic energy of 918.8 ± 0.2 eV, about 1.6 eV higher than that of the Cu_2O peak. This attribution is also consistent with the calculated modified Auger parameter ($\alpha' = E_{K,LMM} + E_{B,2p\,3/2}$), giving the expected value of 1851.3 eV for the metallic Cu. On the other hand, at low overpotentials (−100 and −150 mV) the polycrystalline Cu_2O oxide phase dominates the Auger spectra (insert Fig. 5). For these samples also a higher CuO concentration was determined, which however never exceeded 3 at.%. This phase and traces of $CuSO_4$ show the well-known strong shake-up lines associated with the Cu 2p peak at about 944 eV, observed as small intensity in Fig. 5.

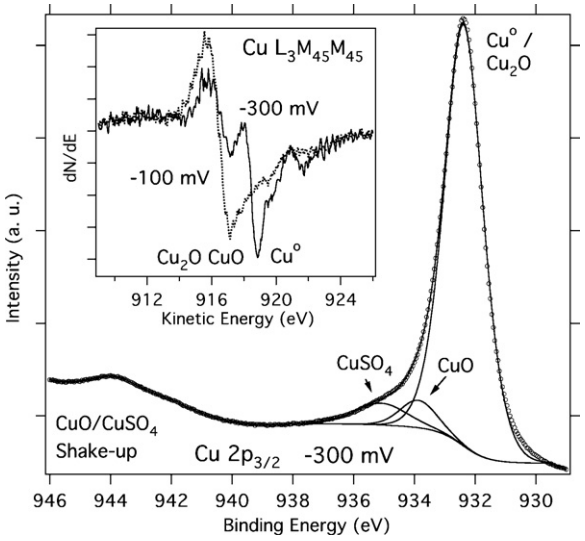

Fig. 5. XPS Cu $2p_{3/2}$ spectrum taken at the bottom side of the AAO film, after Au film removal, for copper deposition at −300 mV. The insert shows the differentiated Auger $L_2M_{45}M_{45}$ spectra for copper deposition at −100 and −300 mV.

The formation of mixed phase $Cu/Cu_2O/CuO$ nanowires by electrochemical deposition into alumina template was reported in several studies.[16–18] Gao et al. pointed out, that for Cu nanowires, prepared by potentiostatic deposition in the range of −150 to −450 mV, smaller negative reduction potentials led to preferential formation of single-crystal structures, avoiding also the formation of oxide impurities.[18] They relate the first effect to the lower nucleation rate in the nanochannels at low overpotentials and the second, to lower rate of OH^- ion production, which leads to copper hydroxide and subsequent copper oxide formation. Considering the potential dependence of oxide formation, our results do not confirm these data. Compared to the later work our results indicate a predominant Cu_2O and CuO phase formation at lower overpotentials, probably due to the high rate of OH^- formation at low reduction currents. In contrast, at higher overpotentials (−250 to −300 mV) a strong decrease of the fraction of oxides and a strong increase of preferential crystalline orientation along the Cu (2 2 0) direction is observed. However, it should be noted, that some divergences regarding the synthesis regime of nanowires with elevated structural order and uniformity might be related to the difference of the electrochemical conditions controlled by the particular structure and geometrical dimensions of the template nanochannels. In our case the data indicate that at higher reduction currents (several mA) the growth of Cu nanowires with a high degree of order along de (2 2 0) direction is promoted. While the growth of dense copper films with (2 2 0) texture by potentiostatic electrodeposition is well known,[19] to our knowledge, the formation of textured copper nanowires was not yet reported in the literature.

4. Conclusions

Anodic aluminium oxide films with polycrystalline hexagonal array of pores and thickness of less than 10 μm presenting nanopore diameter and inter-pore spacing finely tuned by the anodization voltage were prepared. The best ordered periodic arrangement of cylindrical pores was observed for AAO with porosity of about 10%, confirming that the repulsive forces between the neighbouring pores at the aluminium/oxide interface promote the self-organization of the hexagonal pore array.

The electrochemical depositions of Cu in the AAO template result in the growth of continuous metallic nanowires presenting preferential crystalline orientation along the (2 2 0) direction. X-ray diffraction and X-ray photoelectron spectroscopy analyses confirmed also the presence of oxide phases, which proportion decreases strongly at higher overpotentials. The results show that the growth of metallic Cu nanowires with high texture coefficient occurs preferentially in the regime of anodic deposition currents in the mA range.

Acknowledgements

The authors wish to thank FAPESP and CNPq for the financial support and are also grateful to National Laboratory of Synchrotron Light, Campinas, SP, Brazil, for the SAXS and LME for the microscopy facilities.

References

1. Makeevt, M. A., Self-organized quantum dot superstructures for nanoelectronic and optoelectronic applications. *J. Nanoelectron. Optoelectron.*, 2006, **1**, 176–193.
2. Dresselhaus, M. S., Dresselhaus, G. and Eklund, P. C., *Science of Fullerenes and Carbon Nanotubes*. Academic Press, San Diego, 1995, 965p.
3. Cui, Y. and Lieber, C. M., Functional nanoscale electronic devices assembled using silicon nanowire building blocks. *Science*, 2001, **291**, 851–853.
4. Martin, C. R., Nanomaterials: A membrane-based synthetic approach. *Science*, 1994, **266**, 1961–1966.
5. Masuda, H. and Fukuda, K., Ordered metal nanohole arrays made by a 2-step replication of honeycomb structures of anodic alumina. *Science*, 1995, **268**, 1466–1468.
6. Kyotani, T., Xu, W. H., Yokoyama, Y., Inahara, J., Touhara, H. and Tomita, A., Chemical modification of carbon-coated anodic alumina films and their application to membrane filter. *J. Membr. Sci.*, 2002, **196**, 231–239.
7. Masuda, H., Yamada, M., Matsumoto, F., Yokoyama, S., Mashiko, S., Nakao, M. and Nishio, K., Lasing from two-dimensional photonic crystals using anodic porous alumina. *Adv. Mater.*, 2006, **18**, 213–216.
8. Penumetcha, S. S., Kona, R., Hardin, J. L., Molder, A. L. and Steinle, E. D., Monitoring transport across modified nanoporous alumina membranes. *Sensors*, 2007, **7**, 2942–2952.
9. Zach, M. P., Ng, K. H. and Penner, R. M., Molybdenum nanowires by electrodeposition. *Science*, 2000, **290**, 2120–2123.
10. Oh, J. and Thompson, C. V., Selective barrier perforation in porous alumina anodized on substrates. *Adv. Mater.*, 2008, **20**, 1368–1372.
11. Hwang, S.-K., Jeong, S.-H., Hwang, H.-Y., Lee, O.-J. and Lee, K.-H., Fabrication of highly ordered pore array in anodic aluminum oxide. *Korean J. Chem. Eng.*, 2002, **19**, 467–473.
12. Li, F., Zhang, L. and Metzger, R. M., On the growth of highly ordered pores in anodized aluminum oxide. *Chem. Mater.*, 1998, **10**, 2470–2480.
13. Li, D., Jiang, C., Ren, X., Long, M. and Jiang, J., Fabrication of porous anodic alumina membranes with ultrathick barrier layer. *Mater. Lett.*, 2008, **62**, 3228–3231.
14. Nielsch, K., Choi, J., Schwirn, K., Wehrspohn, R. B. and Gösele, U., Self ordering regimens of porous alumina: the 10% porosity rule. *Nano Letters*, 2002, **2**, 677–680.
15. Briggs, D. and Seah, M. P., *Practical Surface Analysis—Auger and X-ray Photoelectron Spectroscopy*. J. Wiley & Sons, Chichester, 1996.
16. Vertegel, A. A., Shumsky, M. D. and Switzer, J. A., Electrochemical growth of a Cu_2O/PbS epitaxial heterojunction on single crystal Au(1 0 0). *Chem. Mater.*, 2000, **12**, 596–598.
17. Wang, M., Zhong, S., Yin, X. B., Zhu, J. M., Peng, R. W., Wang, Y., Zhang, K. Q. and Ming, N. B., Nanostructured copper filaments in electrochemical deposition. *Phys. Rev. Lett.*, 2001, **86**, 3827–3830.
18. Gao, T., Meng, G., Wang, Y., Sun, S. and Zhang, L., Electrochemical synthesis of copper nanowires. *J. Phys. Condens. Matter*, 2002, **14**, 355–363.
19. Guo, D., Zhnag, M., Jin, Z. and Kang, R., Effects of chloride ion on the texture of copper and Cu–ZrB_2 coatings electrodeposited from copper nitrate solution in different plating modes. *J. Mater. Sci. Technol.*, 2006, **22**, 643–646.